Preliminary Design of Aircraft Structures to Meet Structural Integrity Requirements

J. C. Ekvall,* T. R. Brussat,†
Lockheed-California Company, Burbank, Calif.,
A. F. Liu,‡
Rockwell International Corp., Downey, Calif.,
and
Matthew Creager,§
Del West Associates, Inc., Woodland Hills, Calif.

A sample preliminary design analysis is presented illustrating the systematic use of fracture mechanics analysis procedures for sizing aircraft structure to be durable and damage tolerant. A set of damage tolerance design criteria are stipulated, which augment the traditional static and fatigue requirements, to minimize the occurrence of major structural failures in service due to the growth of undetected flaws or cracks. These structural integrity requirements are imposed in a preliminary design analysis for the lower wing surface of a typical fighter/attack aircraft, and the impact of the damage tolerance criteria on design stress and weight is evaluated.

Introduction

RECENT experiences of catastrophic failure on first line military aircraft have focused attention on the engineering criteria used to design and qualify aircraft structures. Generally these catastrophic failures initiated at small cracks in the structure that were not detected by production or in-service inspections. As a result of these experiences the Air Force has been developing new design criteria which will reduce the number of major structural failures due to the presence of undetected damage. To meet these new design criteria the structure must be sized to provide a sufficient subcritical crack growth period and residual strength so that cracks can be detected before reaching a critical size. To properly evaluate preliminary design tradeoffs, structure must be sized to meet these new design criteria as well as fatigue and static strength requirements.

A design study of the lower wing surface of a fighter/attack aircraft was conducted to illustrate how damage tolerance criteria can be considered in preliminary design. The preliminary design procedure utilized in this study is illustrated in Fig. 1. A complete set of design criteria was specified as a basis for the design study. First, baseline designs were developed for three structural configurations made from two materials to meet static strength requirements. Those designs not meeting the fatigue requirements were then resized to a maximum allowable design tension stress based on the results of fatigue analysis. Using fracture mechanics analysis methodology, the final design stress allowables and structural weights were established to meet the damage tolerance requirements. The minimum weight design was then selected which met all the design requirements.

Design Problem

Structure

The wing structure considered is applicable for an approximately 60,000 lb gross weight, high performance fighter/attack aircraft. Typical characteristics for the aircraft selected for this study are given in Table 1. Based on the weight distribution for similar aircraft, the lower wing surface was allocated a target weight of 1480 lb.

The basic structure considered in this study was a multispar wing box with various types of lower skin surfaces. The number of spars was selected to provide the lowest weight within strength and stability constraints using three types of skin surfaces; unstiffened skin, inte-

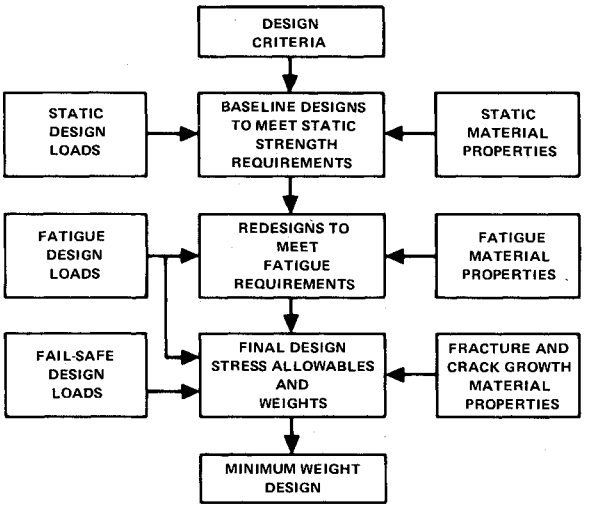

Fig. 1 Flow diagram of preliminary design process to meet structural integrity requirements.

Presented as Paper 73-374 at the AIAA/ASME/SAE 14th Structures, Structural Dynamics and Materials Conference, Williamsburg, Virginia, March 20-22, 1973; submitted April 5, 1973; revision received November 26, 1973. This work was performed under Air Force Contract F33615-71-1324. The authors would like to thank H. A. Wood of the Air Force Flight Dynamics Laboratory for his guidance and encouragement during the course of this study. In addition, the work of the following is gratefully acknowledged; A. C. Jackson for sizing the structure to meet the fatigue and static strength requirements, R. D. Mijares for calculating the wing weights, and P. B. Hamlett for assisting with the crack growth calculations.

Index categories: Aircraft Structural Design (Including Loads), Structural Design, Optimal.

*Design Specialist, Senior, Structural Methods Department. Member AIAA.

†Research Specialist, Structural Methods Department.

‡Member Technical Staff, Airframe Design and Analysis, Space Division.

§Consultant.

Table 1 Typical fighter/attack aircraft characteristics

AIRCRAFT AND WING CHARACTERISTICS	
TAKEOFF GROSS WEIGHT (LB)	58,000
DESIGN GROSS WEIGHT (LB)	52,800
GROSS AREA OF WING (FT^2)	725
ULTIMATE DESIGN LOAD FACTOR	11.00
ASPECT RATIO	4.0
THICKNESS TO CHORD RATIO AT THE ROOT OF WING (%)	6
THICKNESS TO CHORD RATIO AT THE TIP OF WING (%)	6
SWEEP ANGLE AT 25% OF THE CHORD (DEGREES)	35
TAPER RATIO (TIP CHORD DIVIDED BY ROOT CHORD)	0.25
WING WEIGHT (LB)	
UPPER SURFACES, INCLUDING JOINTS AND FASTENERS	2,000
LOWER SURFACES, INCLUDING JOINTS AND FASTENERS	1,480
BEAM WEBS, INCLUDING JOINTS AND FASTENERS	800
RIBS	750
LEADING AND TRAILING EDGES	450
FAIRINGS AND ACCESS DOORS	300
AILERONS	170
LEADING AND TRAILING EDGE FLAPS	800
SPOILERS	100
TOTAL:	6,850

grally-stiffened skin, and zee-stiffened skin. Also the use of both single and multiple-planked skin surfaces was evaluated for the unstiffened skin configuration.

Criteria

Example damage tolerance design criteria selected for this study are given in Table 2. The design must satisfy a fatigue requirement, a durability requirement, and at least one of three alternative structural integrity requirements.

The fatigue and durability requirements relate to the proper choice of material and stress levels, and to the damage that might be present in the delivered aircraft. The intention is to ensure that the basic material resistance to crack initiation and crack growth will be adequate for the chosen stress levels to prevent large numbers of cracks and the necessity of numerous expensive repairs during the lifetime of the aircraft. Specific design details of a particular configuration are not considered.

The purpose of the structural integrity requirements is to ensure the detection and repair of cracks before they can propagate catastrophically. The three alternative criteria reflect three possible means of crack detection. With careful and numerous inspections conducted during manufacture, it is possible to find extremely small cracks in areas that may be impossible to inspect after assembly. Parts in which flaws or cracks are detected can be rejected or repaired. During service thorough periodic inspections are performed, of the order of four times per lifetime, on critical structure with some structure disassembled. If these periodic inspections are done visually for

Table 2 Example damage tolerance and fatigue design criteria

REQUIREMENT	INTITAL CRACK (DAMAGE) SIZE	REQUIRED LIFE OR STRENGTH	SERVICE USAGE	FINAL CRACK SIZE
1. FATIGUE	NONE	4 LIFETIMES	AVG.	NO DETECTABLE CRACKING
2. DURABILITY	.25 INCH (1)	2 LIFETIMES	AVG.	$a < a_{cr}$ (2)
3. STRUCTURAL INTEGRITY SATISFY ONE OF THE FOLLOWING				
3a NON-INSPECTABLE	.050 INCH (1)	2 LIFETIMES	AVG.	$a < a_{cr}$
3b. NDI IN-SERVICE INSPECTABLE	(1) 3-4 INCHES	1 INSPECTION PERIOD	SEVERE	$a < a_{cr}$
3c. WALK-AROUND INSPECTABLE	8-10 INCHES	SUPPORT NOTE (3) LOAD		

(1) THE INFLUENCE OF STRUCTURAL DETAILS ON CRACK GROWTH IS IGNORED FOR THE DURABILITY REQUIREMENT BUT CONSIDERED FOR THE STRUCTURAL INTEGRITY REQUIREMENTS.

(2) a_{cr} = DAMAGE SIZE THAT WILL GROW CATASTROPHICALLY TO FAILURE FOR THE MAXIMUM LOAD IN THE FATIGUE SPECTRUM.

(3) THE ONCE PER 700-FLIGHT MAXIMUM LOAD, PLUS 10% OF CUT LOAD IF INITIAL CRACK CORRESPONDS TO A BROKEN STRUCTURAL ELEMENT.

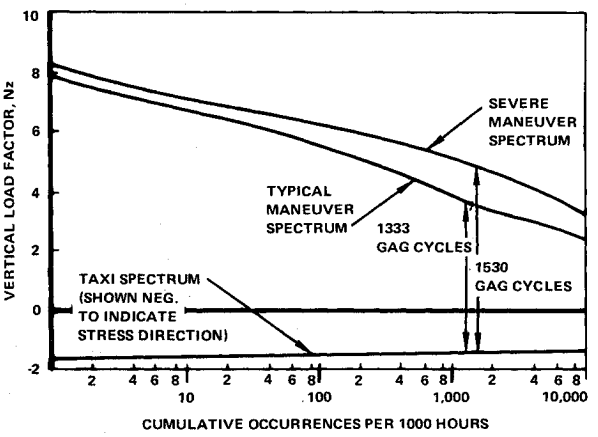

Fig. 2 Fatigue loading spectra for fighter/attack aircraft.

large areas of structure, cracks as large as 3 to 4 in. in length can be missed. Thirdly, before each flight the maintenance and flight crews will perform walk-around inspections of the visible areas of the aircraft. At this time it is possible to miss cracks as large as 8 to 10 in. in length. The rationale behind the specifics of the criteria (that is, initial crack sizes, required lifetimes, etc.) is discussed in Ref. 1.

Design Loads

Design limit loads at the wing root station for this study are as follows:

Shear load = 149,500 lb

Torsional moment about 0.35c = -5.9×10^6 in.-lb

Bending moment = 16.4×10^6 in.-lb

These loads were developed for the wing weight and aircraft characteristics given in Table 1.

Fatigue loading spectra applicable to the lower surface of the wing are shown in Fig. 2. Two spectra were developed from available data for fighter/attack type aircraft to represent typical usage and severe usage. For the fatigue and crack-growth-for-durability analyses, a "mix" spectrum consisting of 75% and 25% of the typical and severe categories, respectively, was used to assure conservatism. The continuous loading spectra were converted to discrete load levels, each described in terms of a maximum and minimum load factor and number of occurrences per 1000 hr. Minimum load factor was +1 for maneuver loads and −1.5 for the ground-air-ground (GAG) cycles; see Fig. 3. GAG cycles were defined in two different ways. For fatigue analysis the GAG cycles were extra cycles having the value that occurs once per flight as shown on Fig. 2. For crack growth analysis the 1333 or 1530 highest positive loads to occur in 1000 hr for the typical and severe spectra, respectively, were taken as the peaks of

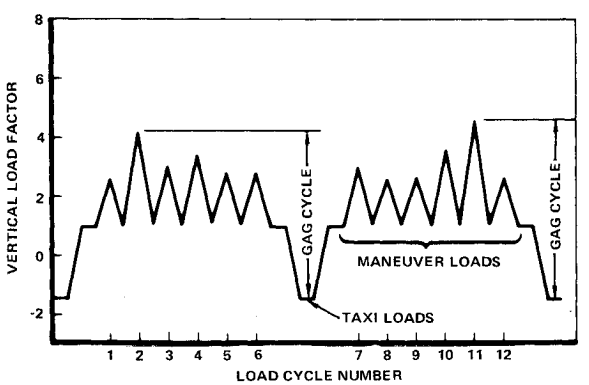

Fig. 3 Sample two-flight-long sequence of cyclic loads.

Table 3 Properties of materials considered for application study

MATERIAL PROPERTIES	PROPERTY VALUES			PROPERTY VALUES/DENSITY		
	D6AC STEEL	Ti6AL-4V	7075-T76 ALUMINUM	D6AC STEEL	Ti6AL-4V	7075-T76 ALUMINUM
F_{tu}, ksi	220	130	69	786	813	690
F_{ty}, ksi	198	126	58	707	788	580
E, 10^3 ksi	29	16	10.3	104	100	103
G, 10^3 ksi	11	6.2	3.9	39	39	39
$F^*_{fatigue}$, ksi	–	47	20	–	294	200
K_{IC} ksi $\sqrt{in.}$	88	63.5	35	314	397	350
K_C**, ksi $\sqrt{in.}$	–	220	85	–	1375	850
K_{ISCC}** ksi $\sqrt{in.}$	22	31	35	79	194	350
*** $K_{10^{-5}}$, ksi $\sqrt{in.}$	22	21.2	16.1	79	133	161
*** $K_{10^{-6}}$ ksi $\sqrt{in.}$	13.5	11	7.8	48	69	78
w, lb./in.^{3}	.28	.16	.10	1	1	1

* R = 0, N = 30,000 cycles K_t = 4.0 for Aluminum and K_t = 5.0 for Titanium

** Maximum value with respect to thickness

*** Stress intensity at 0 to max. loading and crack growth rates = 10^{-5} and 10^{-6} in./cycle

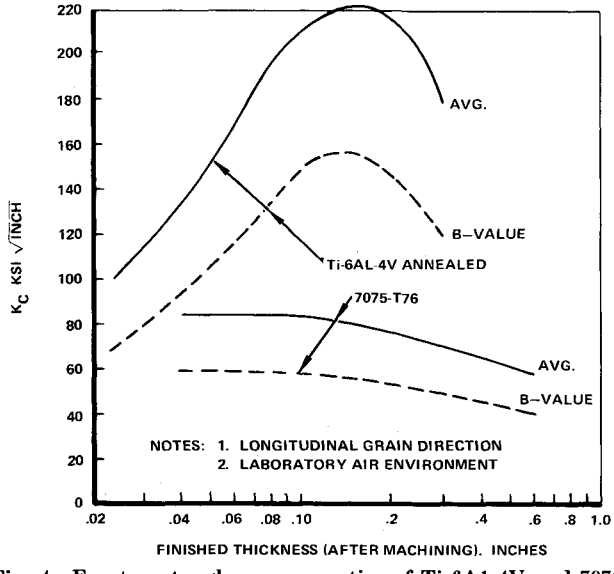

Fig. 4 Fracture toughness properties of Ti-6A1-4V and 7075-T76 aluminum sheet and plate.

GAG cycles instead of maneuver cycles. The first definition is more-or-less standard for fatigue analysis; the second has the advantage of counting each peak load once and only once.

Material Properties

A comparison of the properties for three materials which were considered for the study are given in Table 3. A comparison of these tabulated values and the results of prelminary design analysis indicated that the steel design would be quite heavy; therefore, the design study was limited to Ti-6A1-4V and 7075-T76 aluminum.

The fracture toughness material properties used for the analysis are given in Fig. 4. For the design of reinforced or redundant structure the methods of analysis provide conservative predictions using the average K_c value. For the design of monolithic structure, which does not have effective crack stoppers, more conservative B-values¶ are used

¶MIL-Handbook 5 designation. There is 95% confidence that 90% of the property values will exceed the B property values.

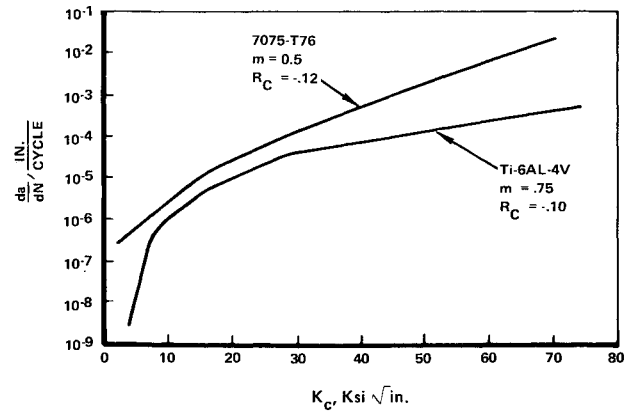

Fig. 5 Constant-amplitude crack growth properties of 7075-T76 aluminum and Ti-6A1-4V.

since reliance is placed on finding the crack by periodic inspections before the crack reaches catastrophic proportions.

For crack growth prediction it must be possible to obtain an expression for stress intensity K, which characterizes the severity of local stresses and deformations at the crack tip. The stress intensity under an applied nominal load** Z is given by

$$K = Z \cdot S \cdot \alpha \tag{1}$$

where S is the ratio of nominal load to nominal stress, and α is the "stress intensity coefficient" which accounts for all configuration effects such as crack length and shape, fastener holes, reinforcements, etc. Expressions for α obtained by elasticity analysis of various configurations are available in the literature.

In general two load magnitudes, a maximum, Z_{max}, and a minimum, Z_{min}, are required to completely describe a fatigue loading cycle. However, a single "effective load" can be defined which describes the fatigue cycle sufficiently to reflect its effect on crack growth. As suggested in Ref. 2, two material constants, m and R_c ($1 \geq m \geq 0$; $R_c \leq 0$), can be determined from crack growth experiments at various Z_{min}/Z_{max} ratios, and effective load is then defined by

$$Z_e = [Z_{max} - \mathrm{MAX}(Z_{min}, R_c Z_{max})]^m Z_{max}^{1-m} \tag{2}$$

where the function MAX(x,y) takes the value of the larger of its two arguments. If conditions of fracture mechanics are applicable, the effective stress intensity ($K_e = Z_e \cdot S \cdot \alpha$) determines the crack growth rate (da/dN) under constant-amplitude cycling in a given material and environment. The K_e vs da/dN curves used in this study are given in Fig. 5. These curves were developed from applicable data for 7075-T6 and 7075-T76 aluminum and Ti-6A1-4V and Ti-8A1-1Mo-1V titanium.

The fatigue and other properties used in the analysis are given in Ref. 1.

Baseline Designs

Static

The baseline designs were developed to meet static strength requirements and then resized to meet the fatigue requirements. The wing designs were analyzed at wing stations spaced at 35-in. intervals from wing root to wing tip. The wing upper surfaces for the skin-stiffened concepts were initially optimized for compression using Emero and Spundt wide column techniques.[3] The unstiffened skin concept was designed so that the upper surface was nonbuckling under compression at limit load. Sizes of basic dimensions for the lower surface of the

**In the present case Z denotes vertical load factor.

Table 4 Structural sizing and stresses to meet fatigue and static requirements for lower wing surface at wing root station

DESIGN CONCEPT	MATERIAL	DIMENSIONS t SKIN IN.	h IN.	t STIFF IN.	b IN.	SPAR CAP AREA IN.2	SPAR SPACING IN.	STRESS FOR ULTIMATE DESIGN LOADS PSI
INTEGRALLY STIFFENED SKIN	7075-T76	.15	2.0	.28	2.0	–	58.5	44,500
	Ti-6AL-4V	.08	1.5	.24	2.0	–	58.5	71,000
ZEE STIFFENERS 4.0 IN ON CENTER	7075-T76	.24	1.5	.20	1.2	–	58.5	44,500
	Ti-6AL-4V	.10	1.25	.10	1.0	–	58.5	92,000
UNSTIFFENED SKIN	7075-T76	.30	–	–	–	1.5	11.7	44,500
	Ti-6AL-4V	.22	–	–	–	1.5	11.7	52,400

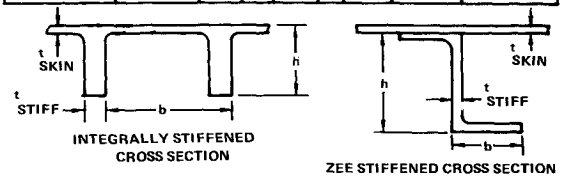

present design were taken to be roughly proportional to the corresponding dimensions of the lower surfaces of comparably-loaded wings from previous designs. These previous designs had been sized to meet static allowable tension stress requirements. The proportionality factor was simply the ratio of the upper surface sizes of the previous and present designs.

Fatigue

Fatigue analysis was performed using the Palmgren-Miner cumulative damage rule, i.e., $D = \Sigma\, n/N$. The load spectra given in Fig. 2 and the relation between load and stress were used to define the fatigue stress spectra. For preliminary design, various stress/load ratios are assumed so that the relation between design stress and fatigue life can be obtained. The fatigue stress spectra and fatigue allowables, in the form of constant-life diagrams, are the input data required for the fatigue analysis.

The constant life diagrams used for the analysis were developed from S-N data in the literature for a K_t value considered appropriate for aluminum and titanium structure. Correlations between fatigue analysis and component fatigue test results indicates that aluminum structures designed to a fatigue quality index of 4 have a high probability of meeting or exceeding the fatigue test requirements. The fatigue quality index is the K_t value of the S-N data that makes $\Sigma\, n/N \equiv 1$ for the test failures analyzed. The fatigue properties of titanium material are generally affected more by fabrication and processing than aluminum materials are and, therefore, a fatigue quality index of 5 was selected. Fatigue tests conducted on titanium structure in connection with the SST program indicates a fatigue quality level of 5 can be achieved.

The results of the fatigue analysis are plotted in Fig. 6. The selected fatigue allowable design stresses reflect the use of a design life of 16,000 hr (4000 hr × 4). The ultimate design stress of 44,500 psi for aluminum is consistent with allowable stresses achieved on current fighter/attack type aircraft. The ultimate design stress of 98,000 psi for titanium structure is above the stresses achieved from static design considerations and, therefore, no resizing was necessary for the titanium structural concepts.

The structural sizing and stresses for the various design concepts are summarized in Table 4 at the wing root station. To illustrate the design procedure and results of the analysis only the data at the wing root station are presented. However, in estimating the wing weights the structural sizing over the full wing span was considered.

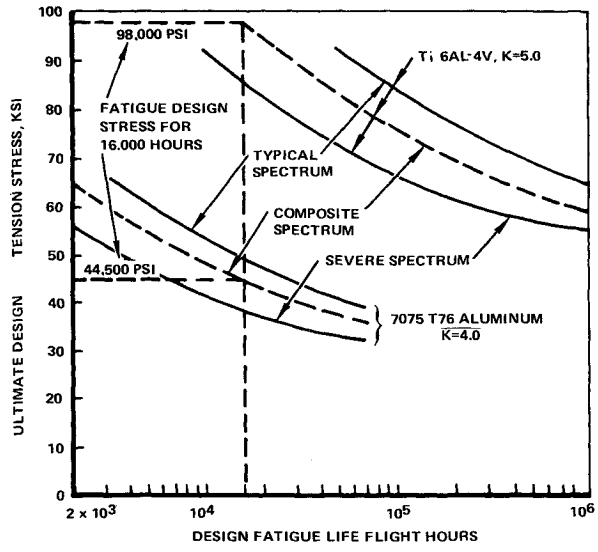

Fig. 6 Fatigue design stresses for Ti-6Al-4V and 7075-T76 aluminum structure.

Design Against Fatigue Crack Growth

Crack Growth Analysis

Fatigue crack growth analyses were conducted to establish ultimate design tension stress allowables to meet the durability requirement and the structural integrity requirements for the noninspectable and NDI inspectable cases.

The process of predicting crack growth under variable-amplitude loading can be divided into two steps. Step 1 is to generate the variable-amplitude crack growth rate curve for a particular material, environment and sequence of loading events. This is a plot of crack growth per flight-hour vs the product $S \cdot \alpha$ [see Eq. (1)]. This step may be bypassed; however, the computational effort saved by this step is enormous. Step 2 is to integrate this curve between an initial and final crack length for each specific configuration and design stress level under consideration.

To calculate crack growth due to a load cycle in a spectrum, the simplest procedure is to assume that the crack growth rate is the same as for constant-amplitude loading. This assumption tends to be conservative, since crack growth under spectrum loading tends to be slower due to the crack-retardation effects of occasional large cyclic stresses. Let the loading spectrum consist of k discrete effective load levels Z_{ei} occurring an average of n_i times per flight-hour, where $i = 1, 2, \ldots k$. For a particular value of the product $S \cdot \alpha$, the growth increment due to a cycle at the ith level is $(da/dN)_i$ as determined from Fig. 5 for an effective stress intensity of

$$K_{e_i} = Z_{e_i} \cdot S \cdot \alpha \tag{3}$$

and the average growth per flight-hour is

$$\frac{da}{dF} = \sum_{i=1}^{k} \left[n_i \cdot \left(\frac{da}{dN} \right)_i \right] \tag{4}$$

By performing this calculation at three selected values of the product $S \cdot \alpha$ and curve-fitting on a log-log basis, the spectrum crack growth rate curve is obtained.

Once the spectrum rate curve has been calculated, the loading spectrum need not be considered further. All required predictions for various crack geometries and various values of S are obtained by numerical integration of this curve. The prescribed configuration of the structure, initial crack geometry, and crack path determine the relationship between crack length and α needed for this calculation. The above approach is explained in detail in Ref. 4.

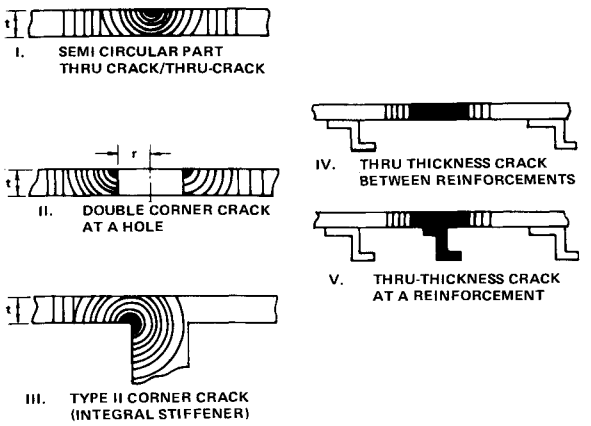

Fig. 7 Elementary geometries for the crack propagation analysis.

Crack growth calculations were conducted for the crack configurations sketched in Fig. 7. The initial crack is shown darkened, and the assumed growth is shown by the striation-type lines. For Cases I through III the part-through crack was assumed to maintain its circular shape until $a = t$. When $a > t$ the crack was assumed to grow as a through-thickness crack of rectangular shape. For cracks in the vicinity of reinforcements, Cases IV and *V*, the effect of the reinforcement was considered in calculating the geometry factor α.

The load-stress conversion factor S at a particular location in a particular design is given by

$$S = (f_{ULT}/Z_{ULT}) \tag{5}$$

where f_{ULT} is the gross area tensile stress at the particular structural location that would result from the application of the ultimate design load factor Z_{ULT}. For the present design study, $Z_{ULT} = 11$. A series of values of S were selected for crack configurations so as to enclose the range of all feasible designs.

The calculated results consisted of plots of crack size versus flight-hours for the various configurations and values of S. These results were considered against the specified damage tolerance criteria to identify stress allowables.

Durability

The design stress allowables required to meet the durability requirement given in Table 2 are shown in Fig. 8.

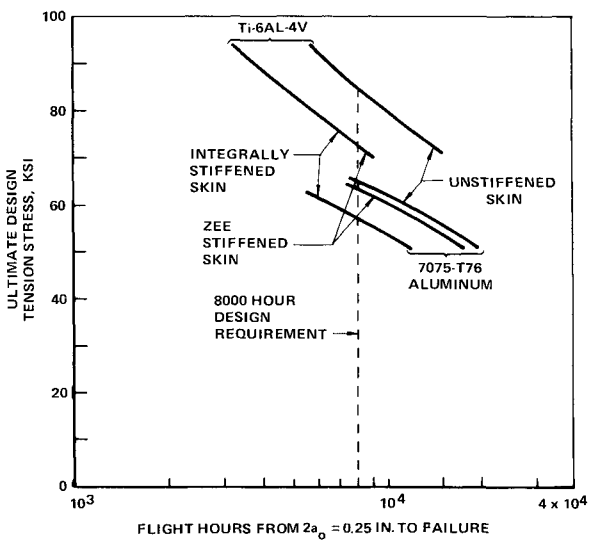

Fig. 8 Design stress allowables to meet the durability requirement.

The ultimate design tension stress must be limited to 57, 63.6, or 65.1 ksi in aluminum structure (depending upon the design concept) and 72.2, 72.2, or 84.8 ksi in titanium structure to prevent an initial flaw ($2a_0 = 0.25$ in.) located anywhere in the skin from reaching a critical size in 8000 flight-hr.

Noninspectable Structure

The criterion for noninspectable structure applies to an initial crack or flaw located at the most critical point in the structure. The critical initial crack is a double corner crack in the skin at the edges of a fastener hole at a reinforcement, Case II of Fig. 7. The reinforcement may be a zee-stiffener or a spar, depending upon the type of construction. Since integrally stiffened structure does not have fastener holes along the reinforcements, a different critical damage must be defined. Two possibilities have been identified. One is a double corner crack at a fastener hole at a skin splice, Case II of Fig. 7. The other is a crack at the internal corner of the integral stiffener, Case III of Fig. 7.

The path or growth sequence of these initial cracks must be anticipated prior to calculation. Some time during the growth process the skin crack located at the fastener hole will cause a crack to initiate in the reinforcement. The time when this will occur is unpredictable, yet it will profoundly affect the crack propagation period that is calculated. As a reasonable compromise of various alternatives, the following crack growth sequence was assumed for the zee-stiffened and multispar unstiffened structure. The initial skin crack is assumed to grow as a double corner crack ($a_0 = 0.05$ in.) until $a = t$. At this point a double corner crack ($a_0 = 0.05$ in.) originates in the stiffener and grows until $a =$ (the thickness of the stiffener). At this point the stiffener breaks. Now the skin crack, which remained stationary while the stiffener crack was propagating, begins to grow again. Its growth is now quite rapid, since the stress field is magnified by the broken stiffener.

For the integrally stiffened cases, there is no problem with crack growth sequence because the structure is continuous. The corner crack is assumed to grow radially until $a = t$, and then as a through-the-thickness crack. Upon reaching the integral stiffener, it is as assumed (based on Ref 5) that the crack grows up the stiffener at the same rate as along the skin.

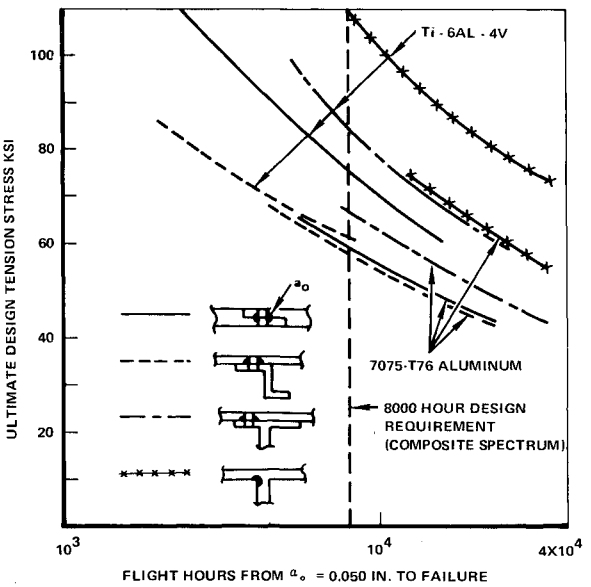

Fig. 9 Design stress allowables to meet the noninspectable structural integrity requirement.

Crack growth periods for the noninspectable structural integrity requirements were calculated based on the above assumptions. The calculations consisted of adding the growth periods for all phases of the growth sequence. The ultimate design tension stress allowables determined from these calculations are given in Fig. 9. To meet the noninspectable requirement, the ultimate design tension stresses must be limited to 58, 59.1 or 66.8 ksi for the three classes of aluminum structure and 61.5, 75.0, or 84.2 ksi for titanium structure. The corner flow in the riser was not as critical as a double corner flaw in one of the fastener holes of the longitudinal skin splice.

NDI In-Service Inspectable Structure

The design criteria for this classification specify that an initial crack located at the most critical point should not grow to catastrophic failure in one inspection period. For the zee-stiffened and 11-spar unstiffened structure, the most critical location of the initial flaw is a through-the-thickness crack at the edge of a fastener hole adjacent to a broken zee-stiffener or spar. For integrally stiffened structure the most critical initial flaw is a through-thickness crack under a partially broken integral stiffener.

The results of the calculations for the NDI in-service inspectable classification are summarized in Fig. 10. Except for the integrally stiffened structure the initial crack size was taken to be r plus (stiffener thickness), where r is the radius of the fastener hole and equal to 0.125 in. A one-inch crack was taken for the integrally stiffened skin structure since this is more comparable to the other cases, i.e., a crack having a total surface length of approximately 3 to 4 in.

The IRAN† inspection interval is generally about 1000 flight hours for fighter/attack type aircraft, i.e., four inspection intervals per lifetime. To achieve this crack growth period the design stress allowables would be limited to 26.7, 32.5, or 38 ksi for the three classes of aluminum structure, and to 38.0, 50.5, or 56.2 ksi for titanium structure. Based on the assumptions made in this analysis, the integrally stiffened structures in both aluminum and titanium provide the highest design allowable stresses for NDI in-service inspectable structure.

Design for Residual Strength

Residual strength analysis is required to size structure to meet the criteria for walk-around inspectable damage. Three types of residual strength analysis were performed. For the unstiffened skin structure, it was assumed that one plank out of ten is broken, with a broken spar cap located in the middle of the broken plank. Thus no crack is present, and the residual strength is determined by relating the stress redistribution due to the broken plank and spar cap to the residual strength of the longitudinal skin splice. For other types of structure the assumed damage is a crack, and classical fracture mechanics can be used as an analytical tool. The three methods of residual strength analysis are discussed below.

Method 1. Skin Crack–Crack Tips Not in the Vicinity of the Reinforcements: This damage case was analyzed for the unstiffened skin structure using a single skin plank the full width of the wing. For this damage case,the residual strength is solely determined by the fracture toughness properties of the skin material. Therefore, the B-basis K_c values, given in Fig. 4, were used in the analysis. The residual strength is calculated simply by the following equation

$$F_g = (K_c/(\pi a)^{1/2}) \qquad (6)$$

To determine the ultimate design tension stress allowables, the stress F_g obtained in Eq. (6) must be related to the appropriate design load, i.e., the once-per-700-flight loads as indicated in Table 2. For the severe spectrum this load occurs once per 455 flight hours or 2.2 times/1000 flight hours for the 34-minute flights. From Fig. 2, this load level corresponds to a vertical load factor of 7.8 g which is approximately 106% limit load. The ultimate design tension stress allowables were then obtained by multiplying the F_g stresses from Eq. (6) by 150/106 = 1.415.

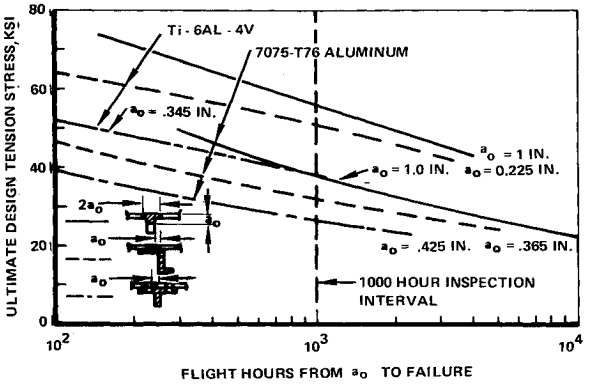

Fig. 10 Design stress allowables to meet the NDI in-service inspectable structural integrity requirement.

Method 2. Skin Crack–Crack Tip in the Vicinity of the Reinforcements: For this damage case, the stress intensity at the crack tip is reduced by the presence of the reinforcement. Therefore, a portion of the cut load is carried by the reinforcements in the vicinity of the crack tips, and the remaining portion by the skin material on either side of the crack. The analysis procedure used for this case is given in Ref. 1. Other residual strength procedures, such as that of Vlieger,[6] would have been equally appropriate. The stress F_g determined from this analysis must be related to the once-per-700-flight design load as discussed above, i.e., multiply $F_g \times 1.415$ to obtain the ultimate design tension stress allowable.

Method 3. One Broken Plank: For the unstiffened structure, the most critical location of the walkaround inspectable damage is centered over a spar cap. If planked construction is utilized, the splice could be located either at a spar cap or midway between spar caps. If the splice is located at a spar cap, then the analysis discussed under 2 above would be utilized. For a splice midway between

Table 5 Design stress allowables to meet the walk-around inspectable structural integrity requirement

TYPE OF STRUCTURE	ASSUMED DAMAGE	METHOD OF ANALYSIS	ULTIMATE DESIGN TENSION STRESS PSI	
			ALUMINUM STRUCTURE	TITANIUM STRUCTURE
UNSTIFFENED SKIN	11.7" a. ONE OUT OF 10 PLANKS BROKEN + A BROKEN SPAR CAP	3	49,300	>68,500*
	11.7" b. 11.7" SKIN CRACK	2	37,400*	113,000
	8" c. 8 IN. SKIN CRACK	1	20,500	58,400
INTEGRALLY STIFFENED SKIN	8"	2	42,900*	102,000*
ZEE STIFFENED SKIN	8"	2	41,600*	115,000*

* THESE DESIGN STRESSES WERE USED TO CALCULATE THE LOWER SURFACE WING WEIGHTS GIVEN IN TABLE 6.

†Inspection as Required And Necessary.

Table 6 Summary of lower surface wing weights to meet various criteria

MATERIAL	TYPE OF STRUCTURE	LOWER WING SURFACE WEIGHT TO MEET VARIOUS DESIGN CRITERIA, LBS.					
					STRUCTURAL INTEGRITY REQUIREMENTS		
		STATIC	FATIGUE	DURABILITY	NON-IN-SPECTABLE	1000 HOUR NDI IN-SERVICE IN-SPECTION INTERVAL	WALK-AROUND INSPECTABLE
ALUMINUM	ZEE-STIFF-ENED SKIN	1240	1564*	1255	1310	2040	1650
	INTEGRALLY STIFFENED SKIN	1375	1564*	1325	1300	1775	1610
	UNSTIFF-ENED SKIN	1817	1830*	①	①	2500	2060
TITANIUM	ZEE-STIFF-ENED SKIN	1338	①	1480*	1655	1955	①
	INTEGRALLY STIFFENED SKIN	1623*	①	1615	1590	1930	①
	UNSTIFF-ENED SKIN	2192*	①	①	①	2770	①

* WEIGHTS THAT MEET ALL REQUIREMENTS

① WEIGHTS LESS THAN REQUIRED FOR STATIC STRENGTH

spars the effective width analysis presented on pp 192–198 of Ref. 7 is used. A design curve developed from test data is used to determine the length required for a given joint design to transfer the load from the broken plank to the adjoining planks. Using this procedure, the fastener strength and spacing is adjusted so as to provide a maximum residual strength consistent with good design practice. The splice used for this analysis was one row of ¼-in. diam steel Hi-Loks with a shear strength of 4650 lb for the aluminum structure, and two rows of the same fastener system for the titanium structure. To obtain ultimate design stress allowables, the design stresses determined from the above analysis must also be related to the once-per-700-flight load. Inclusion of the 10 percent factor (see Table 2) gives an effective redistributed load in the adjacent panels of $[100 + 50 + 0.10(50)]/150 = 1.033$. Therefore, for the broken plank case, the ultimate design tension stresses were obtained by multiplying the stresses determined from the analysis by $1.50/(1.033 \times 1.06) = 1.37$.

The ultimate design tension stress allowables calculated by the residual strength analysis are summarized in Table 5.

The design stress allowable for the multi-spar unstiffened skin structure depends on whether the skin surface is planked or monolithic. If the structure is monolithic, then the allowable stress is 20,500 psi for the aluminum structure and 58,400 psi for the titanium. If the skins are planked, so that the splices occur midway between spar caps, then the design stress allowables could be increased to 37,400 psi for the aluminum structure and 68,500 psi for titanium structure, (the lower stress between cases *a* and *b* in Table 5). For this type of damage, the zee-stiffened and integrally stiffened structure provide higher design stress allowables than the unstiffened skin structure.

Discussion

Environmental Effects

Environmental effects can work in conjunction with either fatigue cycling or sustained tensile load to accelerate the process of deterioration. The choice of baseline data and the calculation procedure used for fatigue and crack growth were affected by a consideration of environmental influences on the fatigue process. The sustained-load effects of environment had to be considered separately.

For the present case a load factor of approximately +1.0 is sustained during flight. No sustained-load crack growth will occur provided the threshold for stress-corrosion cracking, K_{Iscc}, exceeds the sustained stress intensity. Since in both materials K_{Iscc}/K_c exceeds the ratio of the sustained load to the once-per-700-flight load, no sustained-load crack growth is expected.

Evaluation

Lower-wing-surface weights were recalculated so as to individually meet each allowable-stress requirement throughout the span of the wing. Results are given in Table 6.

The minimum weight lower surface that meets all the design criteria is the titanium zee-stiffened skin structure at 1480 lb. It is interesting to note that this exactly meets the target weight given in Table 1 which was established before the analysis was performed. The weight of the titanium zee-stiffened structure had to be increased 10.6% to meet the durability requirement, but it is still 6.4% lighter than the next lightest structure. All the structures can meet one of the three structural integrity requirements without an additional weight penalty. The multispar unstiffened skin structure is not weight competitive with either the zee-stiffened skin or the integrally stiffened skin for this application.

With regard to the three alternative structural integrity requirements, the aluminum structures met the requirement for noninspectable damage whereas the titanium structures met the requirement for walkaround inspectable damage. None of the structures could meet the requirement for NDI in-service inspectable damage for 1000 hr inspection intervals without a large weight penalty. For this criterion to be weight competitive with the other structural integrity requirements, in-service inspections have to be able to detect crack sizes considerably smaller than 3 to 4 in. in length with a high degree of confidence.

It should be emphasized that the results of this sample problem are highly dependent on a number of assumptions and methods of analysis. No testing was done in connection with this study. Therefore the summary presented in Table 6 is by no means a general evaluation of types of structure for fighter/attack aircraft wings.

Conclusions

An application study was performed which consisted of designing the lower wing surface of a fighter/attack aircraft to meet example damage tolerance design criteria. Design stress allowables and structural weights were established for three design concepts for each of two materials. Available analysis methodology was utilized to size

the structure to meet the example criteria. It has been demonstrated that existing methodology is sufficient to permit damage tolerance criteria to be formally considered in the design of primary aircraft structure. The results of the application study indicate that by proper choice of material and design concept, aircraft structure can be designed to meet damage tolerance criteria with little or no weight penalty.

References

[1]Ekvall, J. C., Brussat, T. R., Liu, A. F., and Creager, M., "Engineering Criteria and Analysis Methodology for the Appraisal of Potential Fracture Resistant Primary Aircraft Structure," AFFDL-TR-72-80, Sept. 1972, Air Force Flight Dynamics Lab., Wright-Patterson Air Force Base, Ohio.

[2]Brussat, T. R., "An Approach to Predicting the Growth to Failure of Fatigue Cracks Subjected to Arbitrary Uniaxial Cyclic Loading," *Damage Tolerance in Aircraft Structures,* ASTM STP 486, May 1971, American Society for Testing and Materials, Philadelphia, Pa., pp 122–143.

[3]Emero, D. H. and Spundt, L., "Optimization of Multirib Wing Box Structures Under Shear and Moment Loads," AIAA 6th Structures and Materials Conference, April 1965, Palm Springs, Calif.

[4]Brussat, T. R., "Rapid Calculation of Fatigue Crack Growth by Integration," presented at the 7th National Symposium on Fracture Mechanics, College Park, Md., Aug. 27–29, 1973.

[5]Poe, C. C., Jr., "Fatigue Crack Propagation in Stiffened Panels," *Damage Tolerance in Aircraft Structures,* ASTM STP 486, May 1971, American Society for Testing and Materials, Philadelphia, Pa., pp 79–97.

[6]Vlieger, H. "Residual Strength of Cracked Stiffened Panels," NLR-TR-71004U, Jan. 1971, National Aerospace Laboratory, The Netherlands.

[7]Crichlow, W. J., "The Ultimate Strength of Damaged Structure—Analysis Methods with Correlating Test Data," in *Full-Scale Fatigue Testing of Aircraft Structures,* Pergamon Press, New York, 1960, pp. 149–209.

MARCH 1974 J. AIRCRAFT VOL. 11, NO. 4

Gradient Optimization of Structural Weight for Specified Flutter Speed

E. E. Simodynes*
General Dynamics, Fort Worth, Texas

A method for optimizing structures to satisfy flutter requirements is presented. The specific algorithm employs a gradient of total weight with respect to variable structural parameters as the specified flutter speed remains constant. Equations are derived for direct calculation of the gradient. In applications thus far, the method has been efficient in reducing structural weight while retaining flutter speed without frequent recalculation of normal modes of vibration. An all-movable horizontal tail application is cited in which the skin alone and then the entire structure is resized. Applications using 2 and 6 modes of vibration are also compared.

Introduction

A USABLE flutter optimization method requires a formulation that integrates the contributing analysis disciplines so that the redesign objectives may be attained efficiently and accurately. To accomplish these aims the structural model, the coordinate system, the dynamic representation, the design variables, and the optimization method must be compatible.

The appearance of publications concerned with dynamic optimization of structures indicates an increasing interest in this topic. Turner[1] approached the flutter problem with a method that proportioned structural members so that a specified vibration frequency assumed a given value. The structure attained its required eigenvalues with minimum mass. Other researchers[2-6] have investigated various optimization problems concerned with natural frequencies of structures.

Turner[7] developed a more realistic flutter optimization technique by incorporating aerodynamic forces and the flutter equations into the formulation. Lagrange extremization was used for seeking the configuration of minimum mass. Other researchers[8,9] developed computerized preliminary design programs for considering flutter and also other requirements such as strength and performance. Rudisill and Bhatia[10] developed search procedures using gradient methods. The method was applied to the design of a box beam for a rectangular lifting surface.

In general, resizing a structural component alters the flutter speed and also changes structural "optimality" or efficiency in utilizing structural weight for preventing flutter. The optimization method presented here calculates the gradient of total weight with respect to the variable structural components as the flutter speed remains fixed. It is anticipated that this weight gradient algorithm will be especially convenient when used iteratatively with a method for increasing flutter speed such as the velocity gradient of Ref. 10.

Derivation

With normal mode deflections used as generalized coordinates, the associated unsteady aerodynamic forces $[Q]$ may be calculated with an appropriate aerodynamic theory. The flutter characteristics of the structure are then specified by the following neutral stability equation.

$$([K] - \omega^2[M] - \omega^2[Q])\{q\} = \{0\} \tag{1}$$

Matrix $[K]$ is the generalized stiffness, $[M]$ is the generalized inertia, ω is the flutter frequency, and $\{q\}$ is the complex generalized coordinate vector.

The generalized stiffness and inertia terms are expressed in linear form as

$$[K] = [K^O] + \sum_{j=1}^{n} m_j [K^j] \tag{2}$$

Presented at the AIAA/ASME/SAE 14th Structures, Structural Dynamics, and Materials Conference, Williamsburg, Va., March 20–22; submitted March 29, 1973; revision received November 21, 1973.

Index categories: Aeroelasticity, Structural Design, Optimal.

*Senior Engineer, Structural Dynamics, Convair Aerospace Div.